

# The importance of e+A collisions at an Electron-Ion Collider

Matthew A. C. Lamont (BNL) for the BNL EIC Science Task Force

## Physics Motivation:

- 1) What is the momentum distribution of gluons (and sea quarks) in nuclei?
- 2) What is the space-time distribution of gluons (and sea quarks) in nuclei?
- 3) What is the role of strong gluon fields, parton saturation effects and colour neutral collective gluon excitations in scattering off nuclei?
- 4) Can we experimentally find the evidence of non-linear QCD dynamics in high-energy scattering off nuclei [1]?

## The eRHIC Accelerator Complex

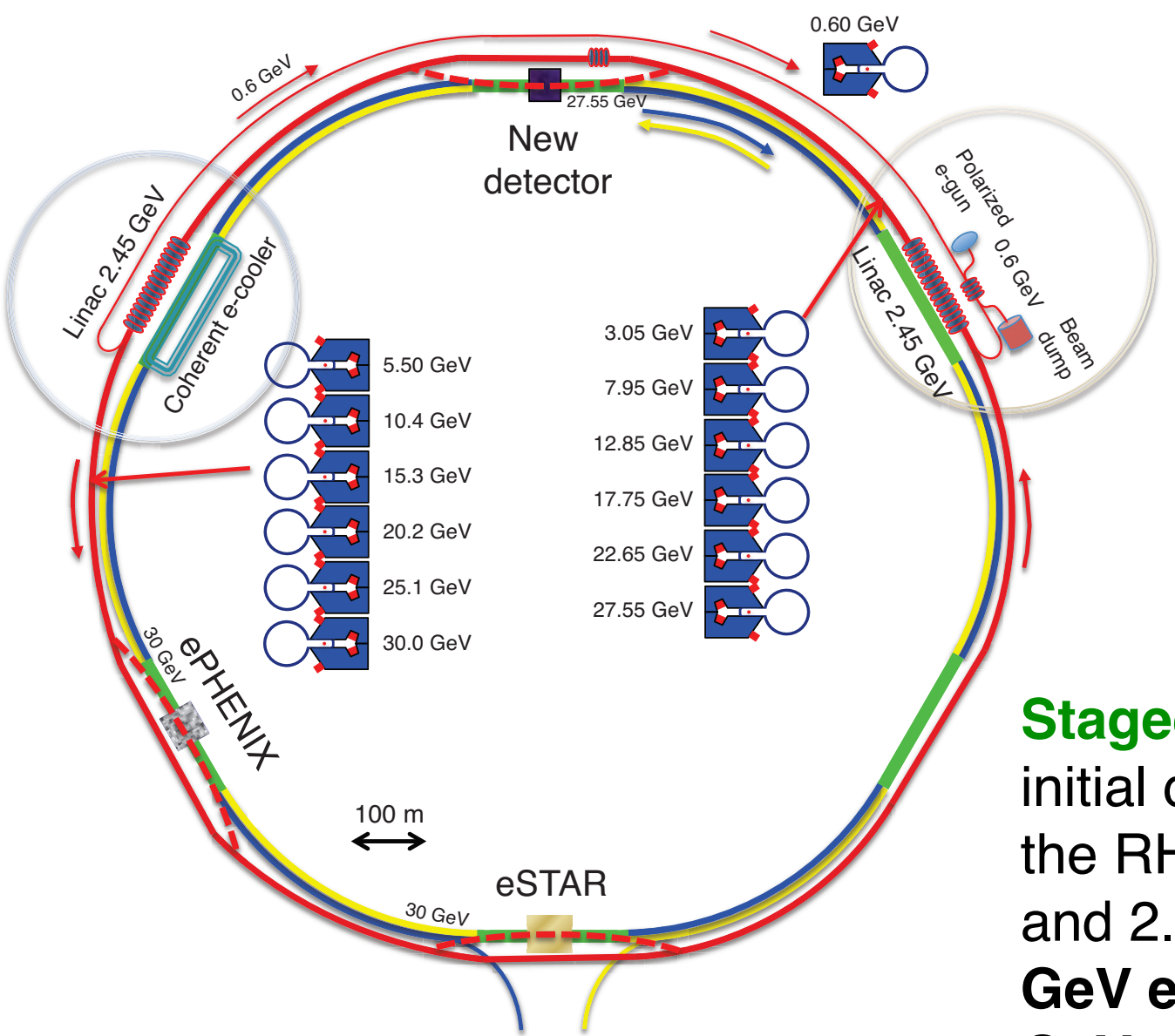


Figure 1: A schematic of the proposed eRHIC accelerator complex

**Multiple Interaction Points:** there is the capability to provide interactions at the current PHENIX and STAR interaction points but importantly, at IP12 where a new detector can be built.

**New Detector:** Upgraded PHENIX and STAR experiments can provide some degree of complementarity. **To complete the physics programme outlined in the poster, it is essential a new detector is built** - fully hermetic using new technologies and based on experience gained from running at HERA.

To achieve the goals laid out in the abstract, a new electron-ion collider will need to be built. The most compelling design is to add a *polarised* electron beam to the current RHIC complex. Its Key Features are:

**Hadron beam energies are those existing at RHIC:** 100 GeV ions, 250 GeV p.

**High luminosities -  $10^{33}$ - $10^{34}$  cm $^{-2}$ s $^{-1}$ :** much higher (~100x) than achieved at HERA, using modern novel technologies such as an energy recovery linac (ERL), crab cavities and high lepton luminosities.

**Staged approach to full energy:** the initial design will have 6 passes through the RHIC tunnel as shown in Figures 1 and 2. A short Linac stage will lead to **5 GeV electrons in stage 1** and up to **30 GeV electrons in a final implementation** when the full Linac is built.

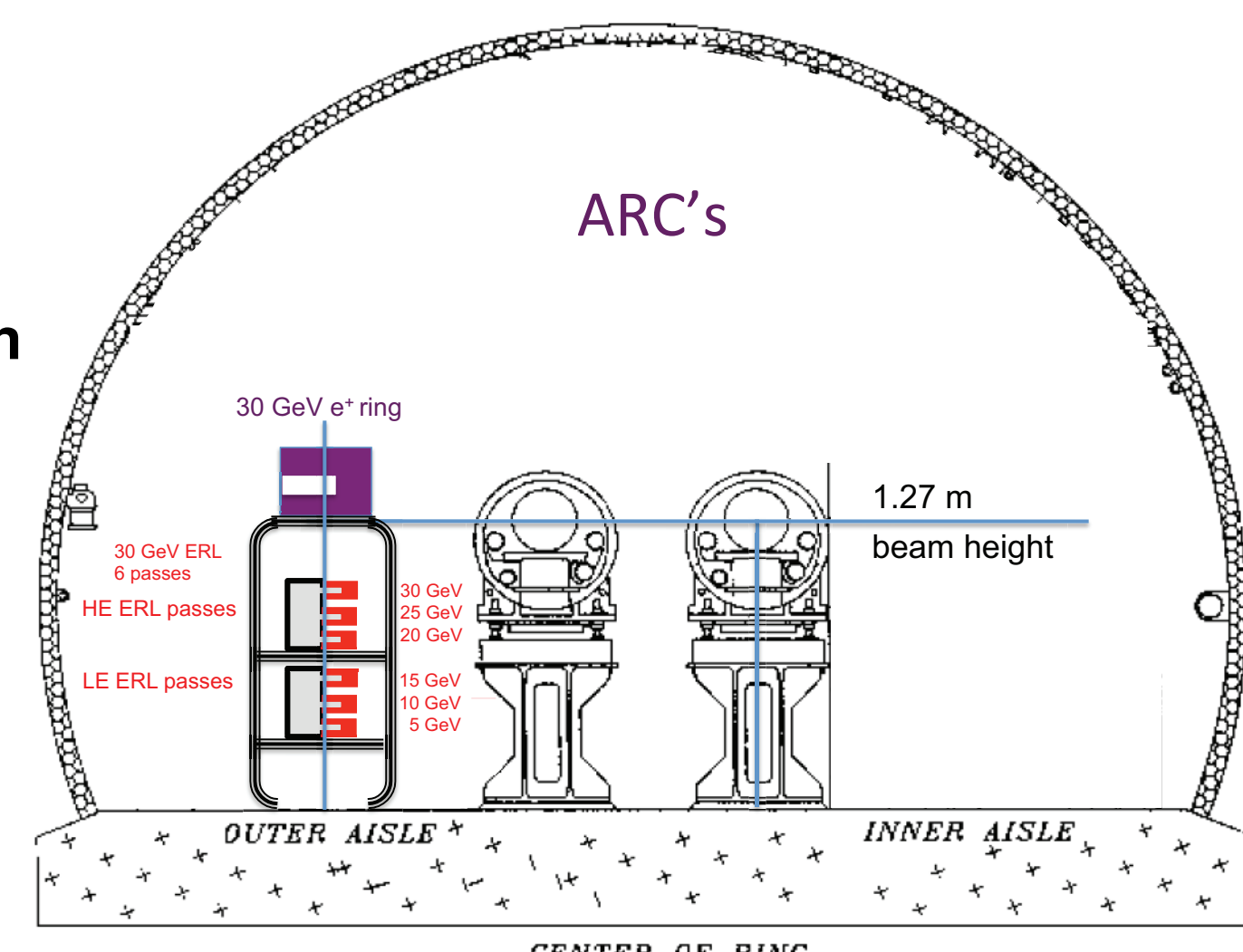


Figure 2: A schematic of how the e- beam fits into the RHIC tunnel

## Deep-Inelastic Scattering

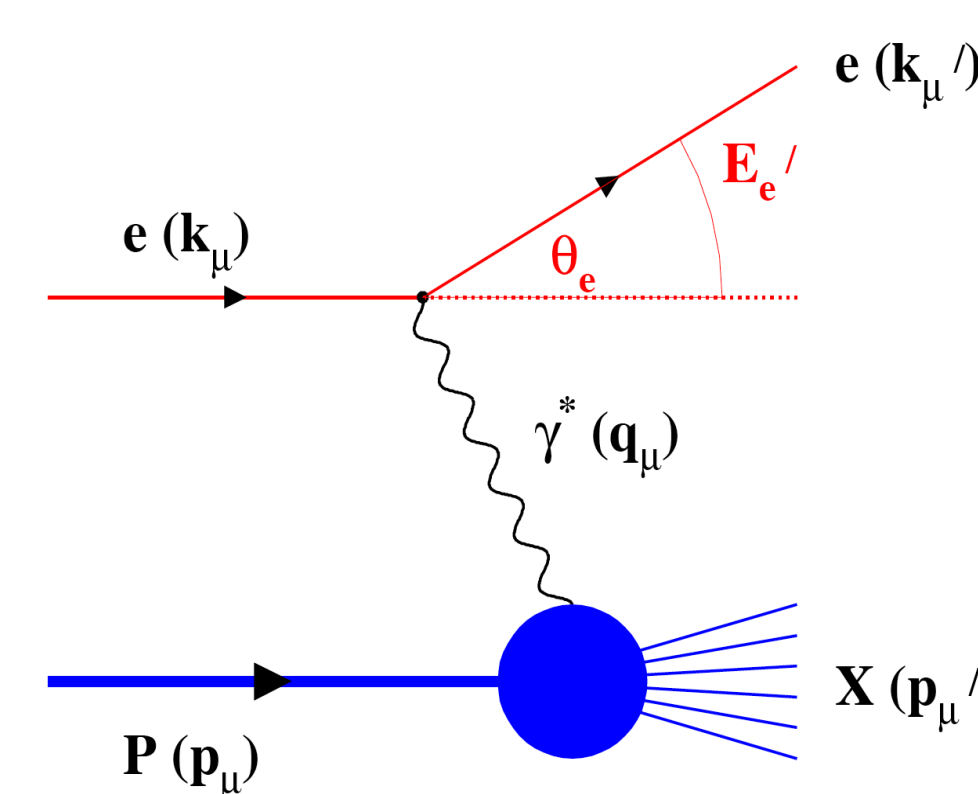


Figure 3: A schematic of a typical DIS event

$$Q^2 = 4E_e E'_e \sin^2\left(\frac{\theta'_e}{2}\right)$$

Measure of resolution power or "Virtuality"

$$y = \frac{pq}{pk} = 1 - \frac{E'_e}{E_e} \cos^2\left(\frac{\theta'_e}{2}\right)$$

Measure of inelasticity

$$x = \frac{Q^2}{2pq} = \frac{Q^2}{sy}$$

Measure of momentum fraction of struck quark

The best way to gain information on the structure of the nucleus is through Deep-Inelastic Scattering (DIS) as outlined in Figure 3. Here, a leptonic probe interacts with the nucleus via the exchange of a virtual photon ( $\gamma^*$ ). The Key Features are:

**Clean probe:** only one interaction in e+A unlike p+A where multiple interactions are possible.

**Kinematics are well understood:** the kinematics of interest, x,  $Q^2$ , y are defined on the left. Note that  $Q^2$  and y can be obtained from a measurement of the outgoing electron. For a given value of  $Q^2$ , one needs to have **higher energy to get to lower x**.

**New kinematic range opened up at eRHIC:** Figure 4 shows the dearth of coverage of current experiments in x,  $Q^2$  space. However, a new set of experiments at eRHIC will greatly expand this to **lower x, even at stage-I**.

**Initial conditions at RHIC, LHC:** the x,  $Q^2$  coverage at eRHIC will allow for a study of cold nuclear matter and the initial conditions at RHIC and the LHC.

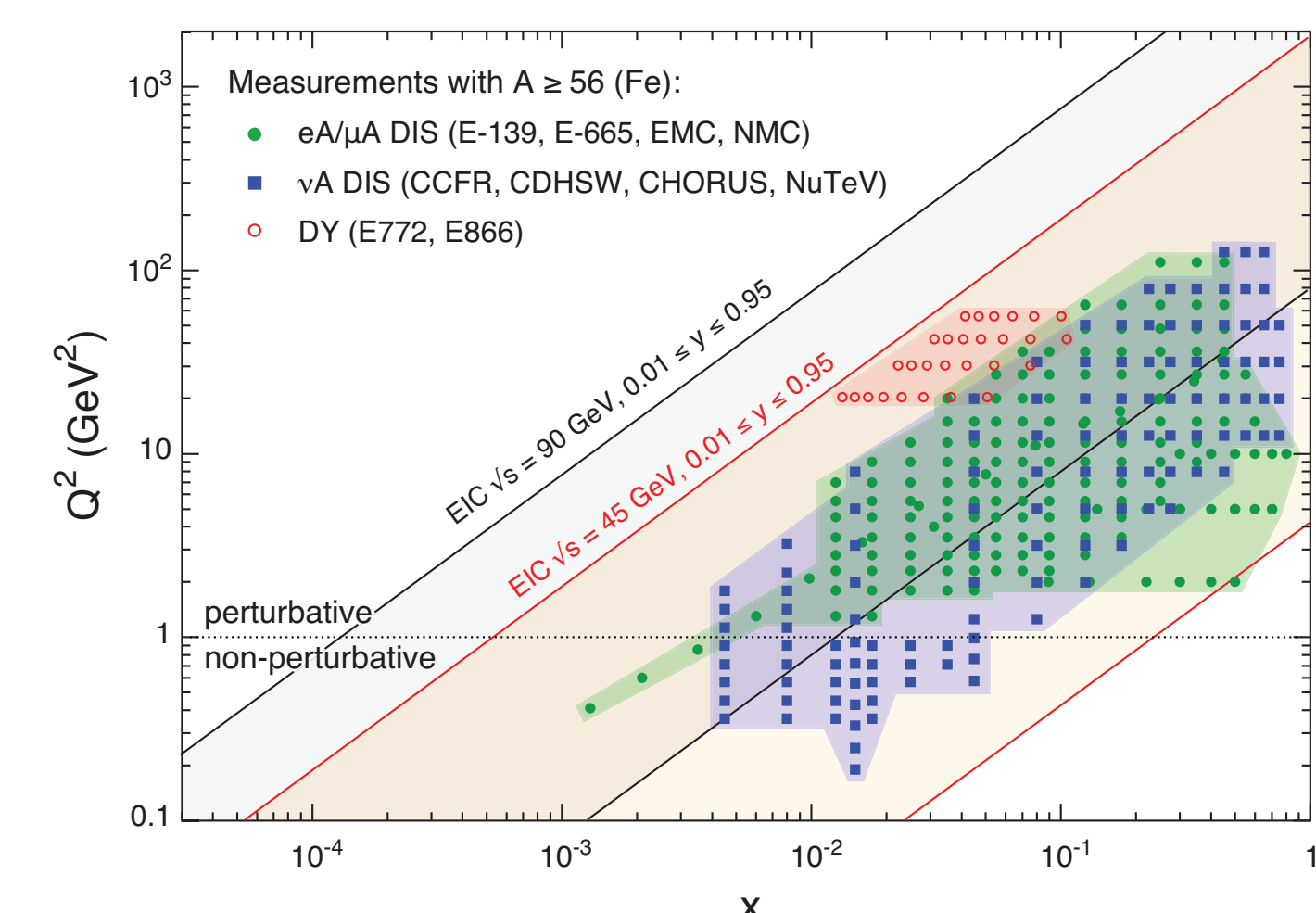


Figure 4: The x,  $Q^2$  coverage of the proposed eRHIC

## Saturation and the Nuclear Oomph Factor

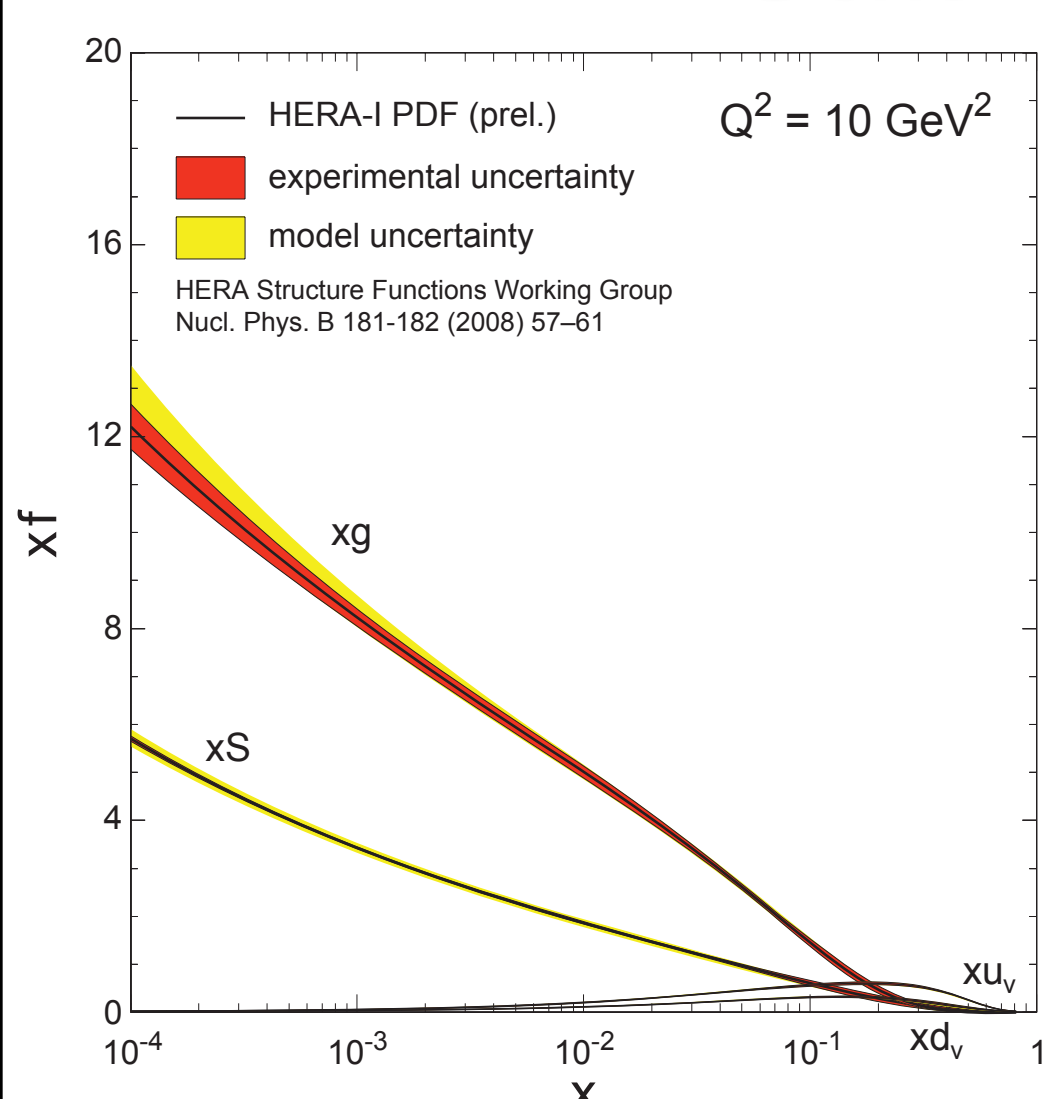


Figure 5: The partonic structure of the proton at  $Q^2=10$  GeV $^2$

Figure 5 shows the result of a linear QCD (DGLAP) fit to e+p DIS data from HERA at  $Q^2 = 10$  GeV $^2$ , which represents the partonic structure of the nucleon as a function of x [2].

**Large gluon contribution at small-x:** whilst the valence quarks dominate, as expected at high-x (~0.3), below  $x=10^{-1}$ , the nucleon is dominated by gluons. This is well described in linear QCD models which describe the growth via gluon splitting.

**Gluon saturation at small-x:** When the density of gluons is large enough, small-x gluons are believed to combine to form higher-x gluons. These processes are described by non-linear QCD equations [3] and encapsulated in the Colour Glass Condensate (CGC) effective field theory [4].

**Saturation scale,  $Q_s^2$ :** The value of  $Q^2$  where these two competing processes are exactly equal and opposite. Saturation occurs for  $Q^2 < Q_s^2$ .

**Nuclear Oomph Factor:** Due to the Heisenberg Uncertainty Principle, low-x gluons interact with the nucleus coherently. Geometric considerations lead to the saturation scale being A-dependent:

$$Q_s^2(x) \sim A^{1/3} \left(\frac{1}{x}\right)^\lambda$$

**Probing saturation at eRHIC:** As shown in Figure 6, the saturation scale for Au is 6x that for protons. The value of x probed in Au is then effectively 100x smaller than for protons in the same energy collisions. Using this feature, we should be able to study saturation physics in nuclei at eRHIC, which wouldn't be possible in e+p collisions.

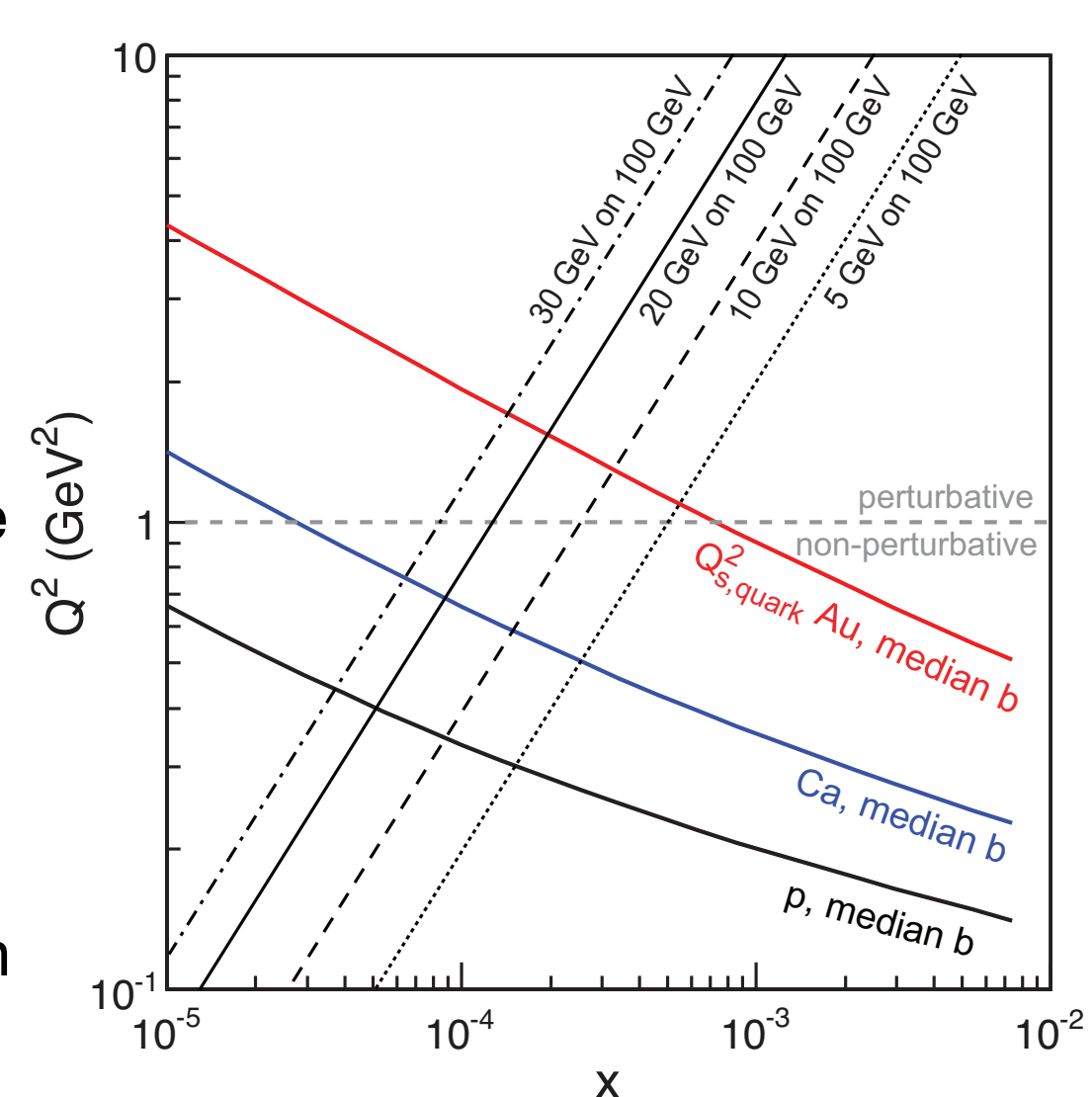


Figure 6: The x,  $Q^2$  dependence of the saturation scale

## Key Measurement: $F_2$ and $F_L$ Structure Functions

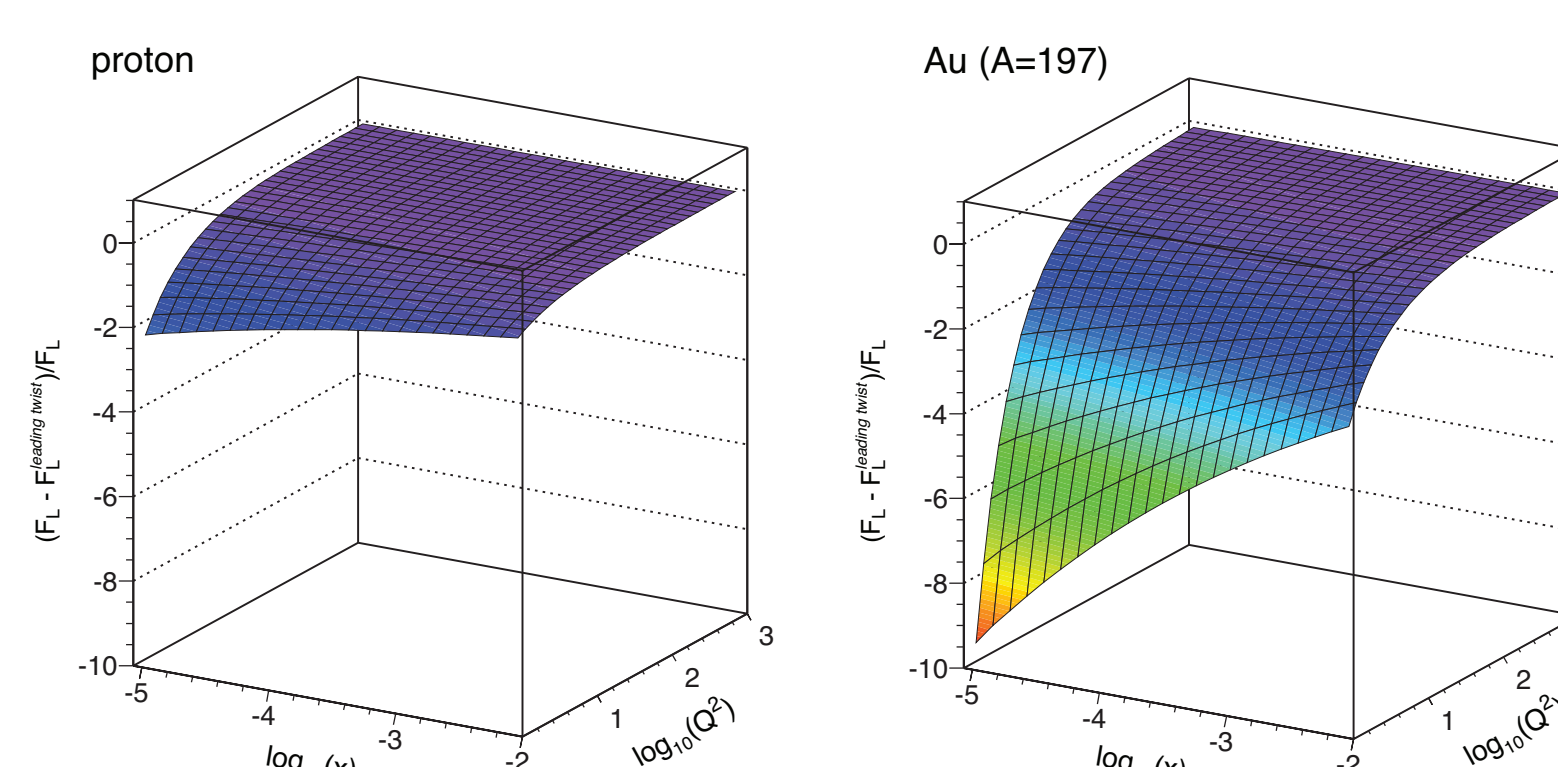


Figure 7: The contribution of higher order processes to  $F_L$  for p and Au

**Sensitivity of  $F_L$  measurements to saturation:** In a saturation model, saturation effects are described by leading twist contributions to  $F_L$ . Figure 7 shows that by plotting the quantity  $(F_L - F_L^{\text{leading twist}})/F_L$  for both protons and Au in the acceptance of eRHIC, saturation effects are much more prevalent in e+Au [5].

**Theoretical uncertainties in  $F_2$ ,  $F_L$ :** Figure 8 shows the current uncertainties in  $F_2$  (left) and  $F_L$  (right) for nuclei for state-of-the-art theoretical models [6], [7]. Whilst  $F_2$  is somewhat constrained by current data,  $F_L$ , which is dominated by gluons, has almost no constraint.

**Experimental uncertainties:** Also shown in Figure 8 are the statistical and systematic experimental uncertainties from 3 months running at 3 different energies. These uncertainties will greatly constrain the different models.

Experimentally, the cross-section for different processes is measured. To learn about the quark and gluon distributions though, we want to calculate the  $F_2$  and  $F_L$  structure functions respectively.

**Reduced cross-section:** By calculating  $\sigma_r(x, Q^2)$ , we can calculate  $F_2^A$  and  $F_L^A$ . To do so, we need get different values of y (where  $Y^+ = 1 + (1-y)^2$ ) which requires **running at multiple energies** then performing a Rosenbluth Separation analysis.

$$\sigma_r(x, Q^2) = F_2^A(x, Q^2) - \frac{y^2}{Y^+} F_L^A(x, Q^2)$$

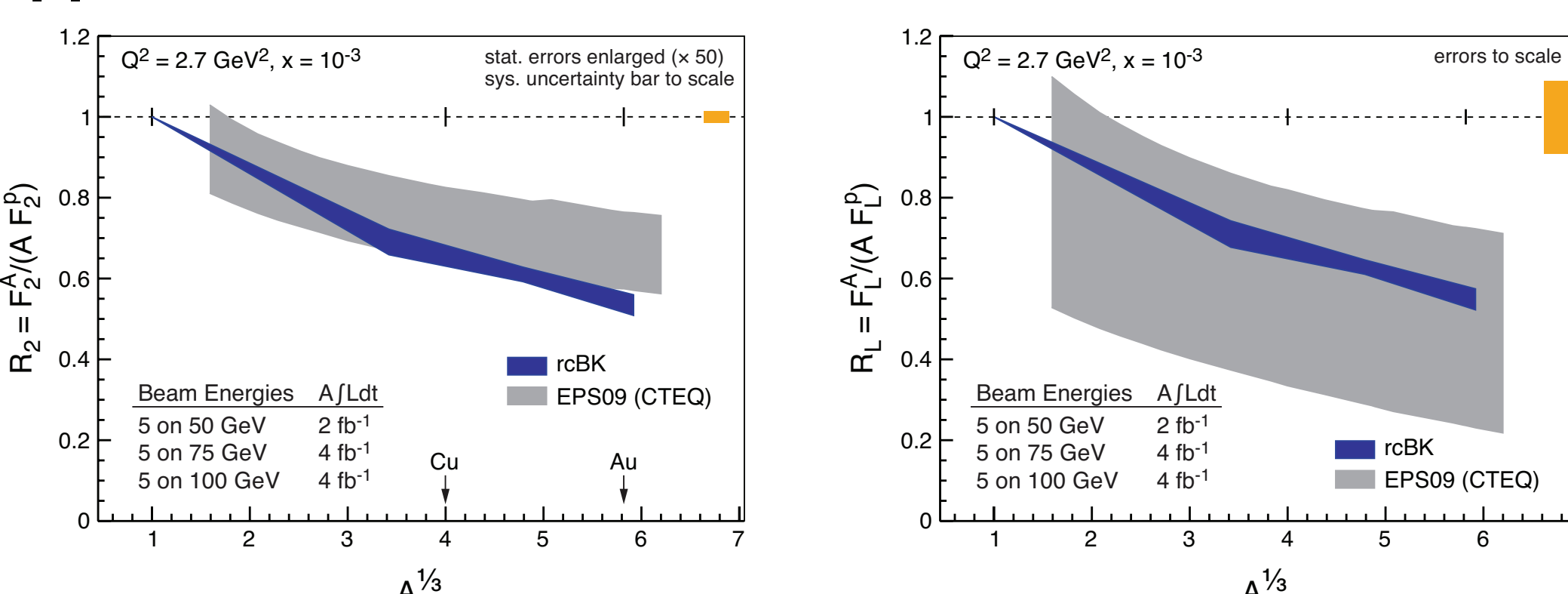


Figure 8: Model predictions for the ratios of  $F_2$  and  $F_L$  for A/p respectively. Also shown are the expected statistical and systematic uncertainties in making the measurement

## Key Measurement: di-hadron Correlations

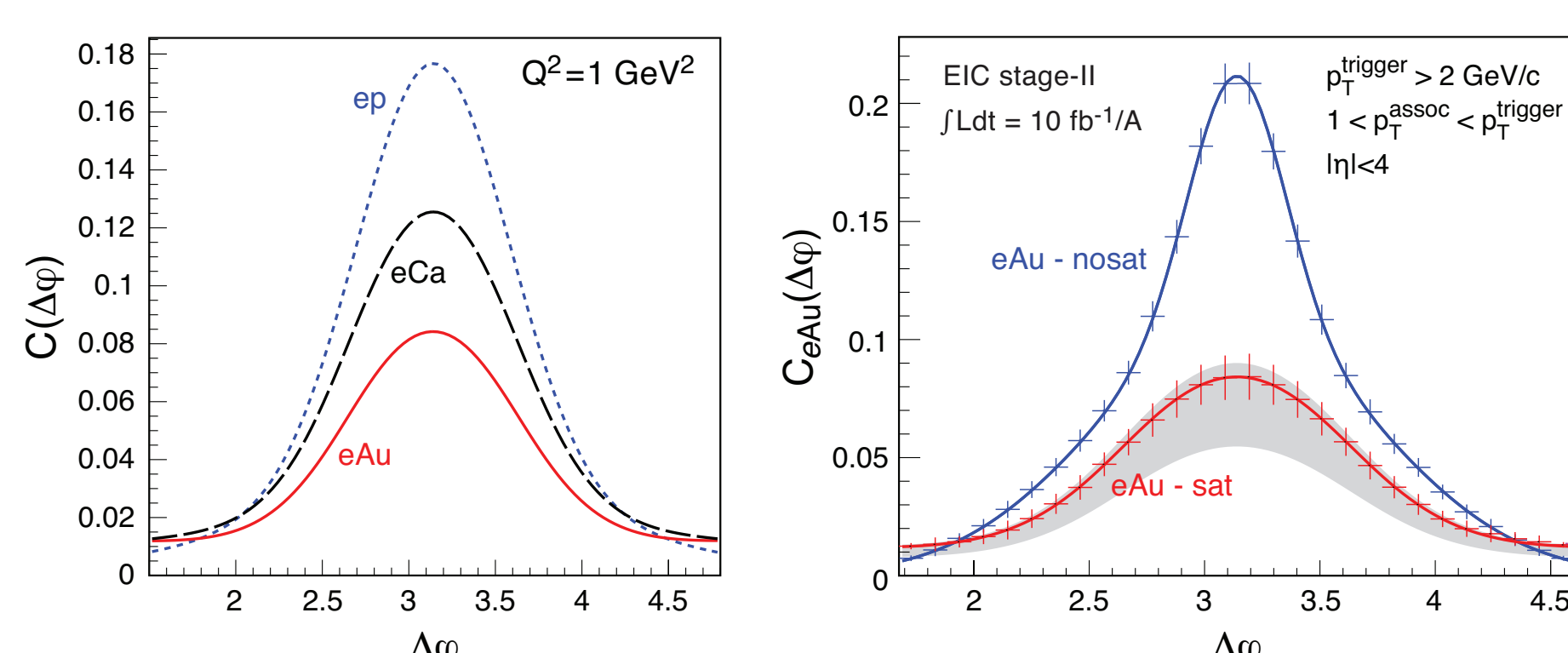


Figure 9: away-side di-hadron correlations in e+A vs e+p in a saturation model together with predicted error bars for 6 months of running at eRHIC

**Theoretical interpretation:** This suppression in forward d+Au collisions has been explained by a saturation model. However, the lack of exact knowledge of the kinematics means that this is difficult to interpret.

**Correlations in e+A:** Figure 9 shows model predictions on the left for the A dependence of the suppression. On the right, experimental error bars show that predictions from saturation and non-saturation models can be distinguished.

**$J_{eAu}$  - relative yields:** Figure 10 shows the capabilities for measuring  $J_{eAu}$  at eRHIC - the relative yield of back-to-back hadron pairs between e+Au and e+p collisions. Also shown is the measurement from PHENIX for d+Au collisions [8]. The comparison to theory is again complicated by the lack of knowledge of the kinematics of the collision.

One of the highlights of the RHIC physics programme to date has been the suppression of away-side di-hadron correlations at mid-rapidity in Au+Au collisions.

**mid-rapidity d+Au:** At mid-rapidity in d+Au collisions, no suppression was observed in away-side di-hadron collisions. This lead to the interpretation that the suppression was due to energy loss in a final-state de-confined medium.

**forward d+Au suppression:** The same measurement was performed using forward di-hadrons in d+Au. This time, a suppression was observed.

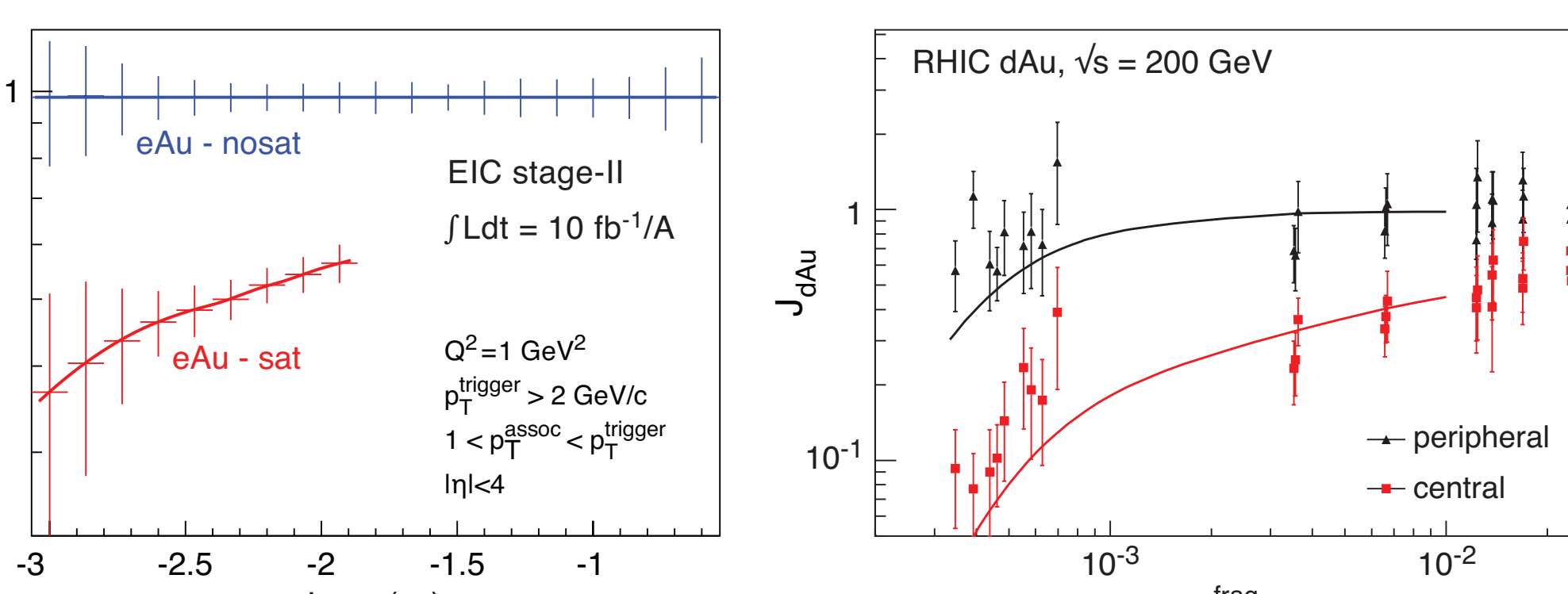


Figure 10:  $J_{eAu}$  predictions at eRHIC in a saturation model

## Key Measurement: Diffraction

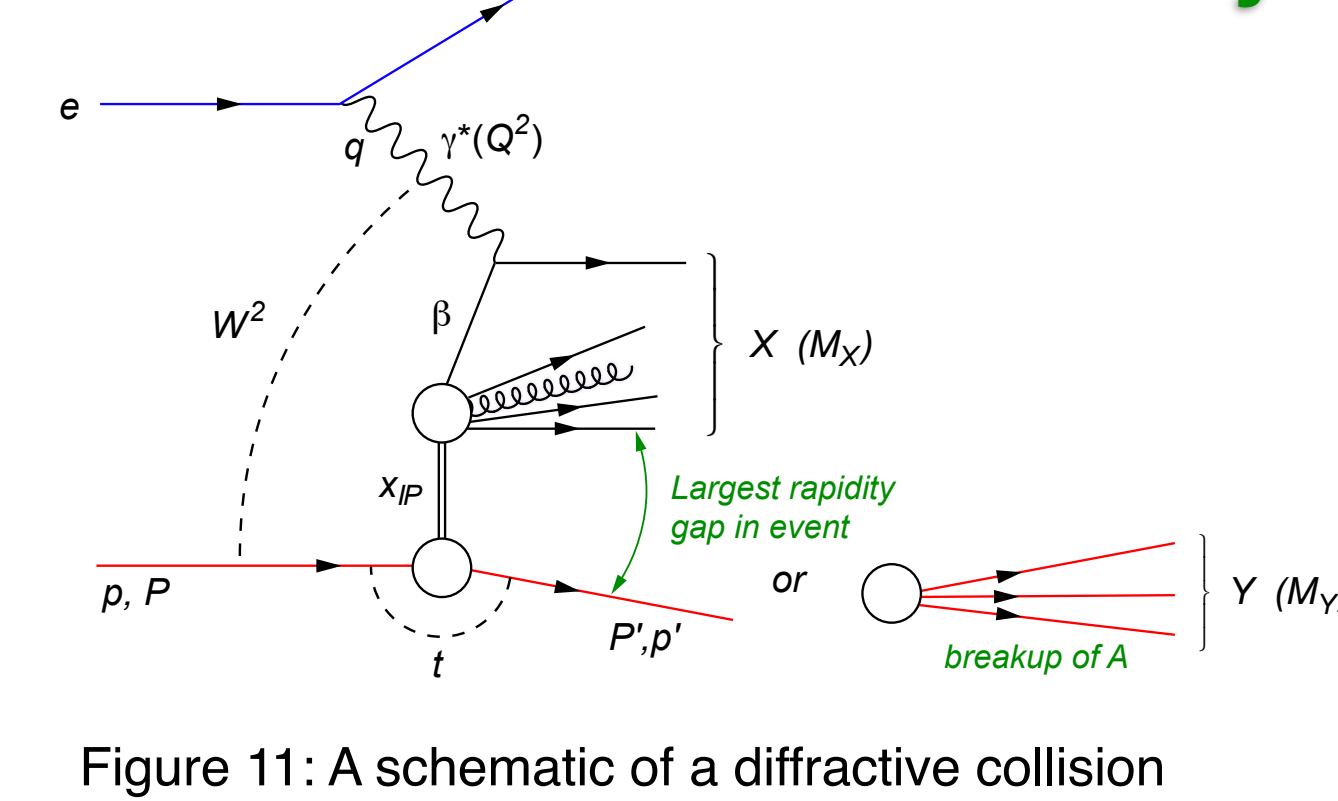


Figure 11: A schematic of a diffractive collision

As well as DIS, diffractive collisions are also of interest. That is, the electron probe interacts with a colour-neutral excitation in the nucleus (often called a Pomeron) as shown in Figure 11 and there is then a gap in rapidity of produced particles.

**Large fraction of cross-section:** At HERA, diffractive events were found to make up 10-15% of the cross-section. Predictions for e+Au at eRHIC put this as high as 30-40%.

**High sensitivity to the gluon distribution:** Diffraction is the most sensitive measure we have of gluons - it is proportional to the square of the gluon distribution

**Two classes of diffractive events:** coherent diffraction, where the final state nucleus remains intact and incoherent diffraction, where the nucleus breaks up. **Coherent diffraction is sensitive to the spatial gluon distribution and incoherent diffraction is sensitive to fluctuations in the gluon distribution.**

**Experimentally challenging:** Unlike e+p, the nucleus cannot be measured in a forward spectrometer. Coherent diffractive events are then those where a rapidity gap is measured in the detector and no break-up neutrons are measured in a zero-degree calorimeter.

**Exclusive Vector Meson Production:** Figure 12 shows the diffractive rho-meson distribution as a function of the momentum transfer. Coherent diffraction is dominant at small-|t|. The experimental error bars will be able to distinguish between saturation and non-saturation models. **The incoherent distribution will be able to be suppressed experimentally to enable the measurement of the first 3 minima in the coherent distribution.**

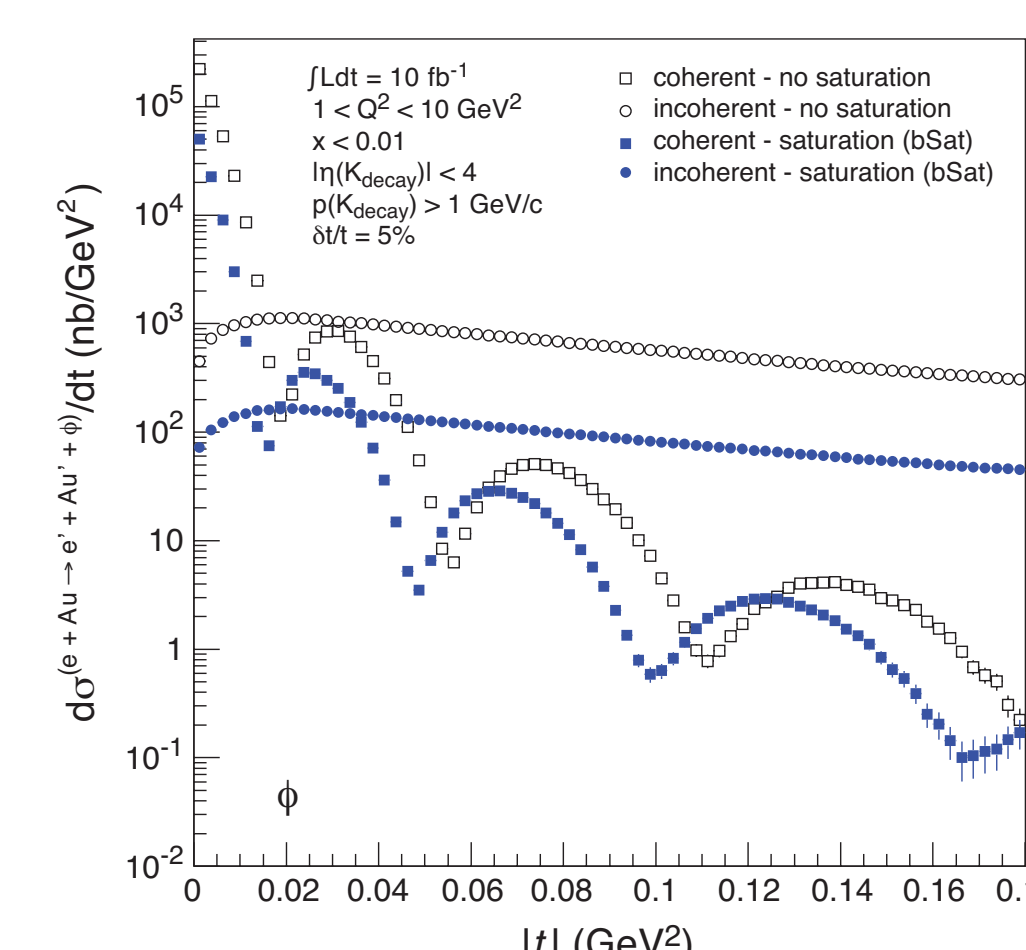


Figure 12: |t| distribution of the  $\phi$  meson in coherent and incoherent diffractive events

- [1] "Gluons and the quark sea at high energies: Distributions, polarization and tomography," Eds D. Boer, M. Diehl, R. Miller, R. Venugopalan, W. Vogelsang, BNL-96164-2011, INT-PUB-11-034, JLAB-THY-11-1373
- [2] HERA structure functions working group, Nucl. Phys. **B181-182** 57-61 (2008)
- [3] J. Jalilian-Marian, A. Kovner, A. Leonidov, and H. Weigert, Phys. Rev. **D59**, 014014 (1998)

- [4] E. Iancu, A. Leonidov, and L. D. McLerran, Phys. Lett. **B510**, 133 (2001)
- [5] J. Bartels, K. Golec-Biernat, and L. Motyka, Phys. Rev. **D81**, 054017 (2010)
- [6] J. L. Albacete, N. Armesto, J. G. Milhano, and C. A. Salgado, Phys. Rev. **D80**, 034031 (2009)
- [7] K. J. Eskola, H. Paukkunen, and C. A. Salgado, JHEP **04**, 065 (2009)
- [8] PHENIX Collaboration, A. Adare et al., Phys.Rev.Lett. **107**, 172301 (2011)